International Journal of Nanomedicine

Dovepress
Taylor & Francis Group

Open Access Full Text Article

ORIGINAL RESEARCH

MiRNA Let-7i-5p-Contained Small Extracellular Vesicles from Macrophages Induce Nucleus Pulposus Cell Senescence via Targeting LIN28A

Shuo Zhang[1,2,*], Miaoheng Yan[3,*], Xiao Lv[2,*], Peng Wang[2], Weijian Liu[2], Binwu Hu[2], Songfeng Chen[3], Zengwu Shao[2]

[1]School of Medicine, Nankai University, Tianjin, 300071, People's Republic of China; [2]Department of Orthopaedics, Union Hospital, Tongji Medical College, Huazhong University of Science and Technology, Wuhan, 430022, People's Republic of China; [3]Department of Orthopaedics, The First Affiliated Hospital of Zhengzhou University, Zhengzhou, 450052, People's Republic of China

*These authors contributed equally to this work

Correspondence: Songfeng Chen, Department of Orthopaedics, The First Affiliated Hospital of Zhengzhou University, Zhengzhou, 450052, People's Republic of China, Email fccchensf@zzu.edu.cn; Zengwu Shao, Department of Orthopaedics, Union Hospital, Tongji Medical College, Huazhong University of Science and Technology, Wuhan, 430022, People's Republic of China, Email szwpro@163.com

Purpose: To investigate the role of macrophage-derived small extracellular vesicles (MΦ-sEVs) in nucleus pulposus (NP) cell (NPC) senescence and screen the pro-senescent micro-RNA (miRNA) in MΦ-sEVs and potential mRNA targets.

Methods: Bone marrow-derived macrophage (BMDM)-derived sEVs were isolated by differential centrifugation, and the phenotypes of MΦ-sEVs were identified. NPCs were treated with MΦ-sEVs, and cellular senescence levels were examined by senescence-associated β-galactosidase (SA-β-Gal) staining and Western blotting (WB). Activation of the senescence-associated secretory phenotype (SASP) was tested using qRT-PCR and cytometric bead arrays (CBA). LPS+IFNγ-MΦ-sEVs or IL-4-MΦ-sEVs were injected into the rat coccygeal NP tissues to determine the in vivo effects of MΦ-sEVs on intervertebral disc degeneration (IVDD) and NPC senescence. The miRNA levels in MΦ-sEVs were evaluated using PANDORA sequencing. NPCs were transfected with miRNA mimics or inhibitors to screen the miRNAs with pro-senescence effects.

Results: MΦ-sEVs displayed the cup-shaped morphology, with diameters mainly ranging from 40 to 200 nm. Both LPS+IFNγ-MΦ-sEVs and IL-4-MΦ-sEVs impaired NPC viability and accelerated NPC senescence. The expression levels of SASP and senescence-related proteins, including p16, p21, and p53, were elevated by MΦ-sEVs treatment. Animal experiments indicated that LPS+IFNγ-MΦ-sEVs or IL-4-MΦ-sEVs exacerbated IVDD with increased p16-positive cell ratio and activated SASP. PANDORA sequencing of MΦ-sEVs revealed high levels of let-7i-5p, which exerted pro-senescence effects by downregulating LIN28A expression. Inhibiting or silencing LIN28A by C1632 or specific siRNAs also triggered NPC senescence.

Conclusion: Both LPS+IFNγ-MΦ-sEVs and IL-4-MΦ-sEVs induced NPC senescence by delivering miRNA let-7i-5p to inhibit LIN28A.

Keywords: macrophage-derived small extracellular vesicle, intervertebral disc degeneration, nucleus pulposus cell, senescence, let-7i-5p

Introduction

Intervertebral disc (IVD) degeneration (IVDD) is a common musculoskeletal disorder characterized by the overactivation of inflammatory response and extracellular matrix (ECM) catabolism.[1,2] Our previous studies have suggested that macrophage infiltration is extensively involved in IVDD pathogenesis.[3,4] M1-type macrophages exasperated inflammatory cascades and triggered senescence of nucleus pulposus (NP) cells (NPCs),[3,5] whereas M2-type macrophages promoted NP fibrosis and pathological angiogenesis.[6] Other researches demonstrated that the conditioned medium (CM) of M2-type macrophages could exert cytoprotective effects on NPCs.[7,8] In consideration of the complex

Received: 14 June 2024
Accepted: 25 January 2025
Published: 18 February 2025

Graphical Abstract

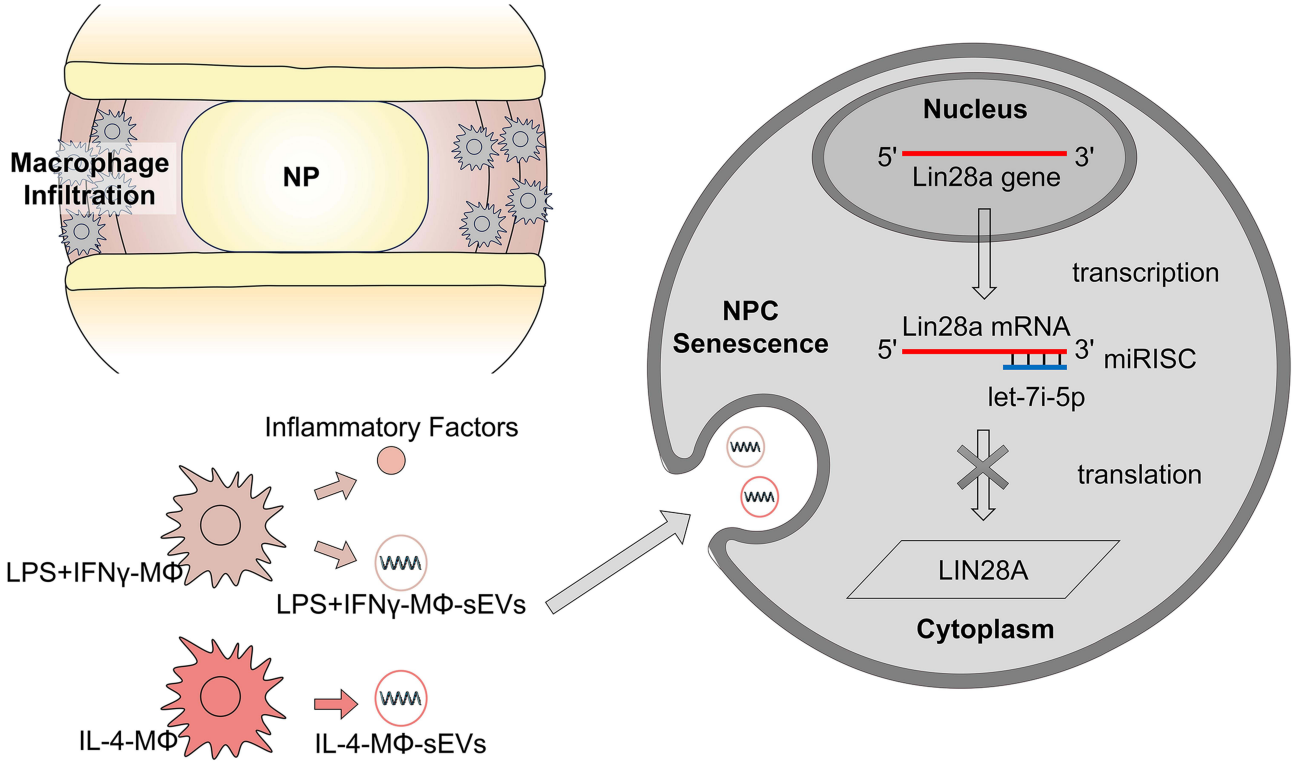

phenotypic characteristics of macrophages, it is essential to further investigate the interactions between macrophages and NPCs in degenerated IVD tissues.

Small extracellular vesicles (sEVs), which are crucial cell communication messengers, can deliver various contents, including nucleic acids, proteins, and metabolites, into recipient cells and effectively regulate complex signaling pathways.[9] Macrophage-derived sEVs (MΦ-sEVs) are implicated in the pathogenesis of multiple inflammatory diseases, such as osteoarthritis (OA) and periodontitis.[10,11] Micro-RNA (miRNA), a kind of conserved non-coding RNA, usually serves as sEV cargos and widely participates in post-transcriptional regulation.[12,13] MiRNAs can impede target gene translation by directly binding to the 3'-untranslated region (3'-UTR) of mRNA to form miRNA-induced silencing complex (miRISC).[14,15] In IVD tissues, various miRNAs are involved in cell apoptosis, proliferation, ECM metabolism, and inflammatory response activation.[16] However, the effects and mechanisms of MΦ-sEVs on IVD physiology and pathology have not been fully elucidated.

Cellular senescence, mainly caused by DNA damage and telomere shortening, is featured with irreversible cell cycle arrest and senescence-associated secretory phenotype (SASP) activation.[17] Studies have shown that the proportion of senescent NPCs significantly increases with the IVDD degree. Senescent NPCs can exasperate inflammatory response and ECM catabolism, impair ECM anabolism, and thus accelerate the IVDD process.[18,19] The tumor suppressor protein p53-p21 (cyclin-dependent kinase inhibitor 1A, CDKN1A)-retinoblastoma protein (Rb) pathway and p16 (cyclin-dependent kinase inhibitor 2A, CDKN2A)-Rb pathway are the main signaling pathways that regulate IVD cell senescence.[19]

Considering all of the evidence, it was hypothesized that MΦ-sEVs could regulate NPC senescence. In this study, the impacts of MΦ-sEVs on NPC senescence were investigated, and small RNA sequencing was conducted to screen the potential miRNAs. In addition, the current study further explored the cytoprotective effects of interleukin (IL)-4-treated MΦ on NPC.

Materials and Methods

Preparation of Bone Marrow-Derived Macrophages

Rat bone marrow-derived macrophages (BMDMs) isolation, in vitro culture, and polarization were performed as previously reported.[6] BMDMs were treated with 100 ng/mL lipopolysaccharide (LPS) (Beyotime, Shanghai, China) and 25 ng/mL rat interferon-γ (IFN-γ) (GenScript, Nanjing, China) for 24 h (LPS+IFNγ-MΦ), or 30 ng/mL rat IL-4 (PeproTech, Rocky Hill, NJ) for 24 h (IL-4-MΦ). After polarization, rat BMDMs were identified by flow cytometry (FCM) using anti-CD32, FITC-conjugated anti-CD11b/c, APC-conjugated anti-CD68, BV421-conjugated anti-CD86, and PE-conjugated anti-CD206 antibodies. The antibodies used in this study are listed in Table S1. Bulk RNA sequencing (RNA-seq) was further performed to identify the phenotypic characteristics of BMDMs.

Isolation and Identification of Macrophage-Derived sEVs

MΦ-sEVs were isolated from the cell culture supernatant by differential centrifugation as previously described.[20] Briefly, BMDMs were cultured in the EV-free medium for 48 h. The conditioned medium (CM) was harvested and centrifuged at 300 × g for 10 min, at 2×10^3 × g for 10 min, and at 10^4 × g for 30 min. The supernatant was ultracentrifuged at 10^5 × g for 70 min (Beckman Coulter, Brea, CA, USA). The sEVs pellet was resuspended in phosphate-buffered solution (PBS) and ultracentrifuged at 10^5 × g for another 70 min to remove contaminating proteins. All the steps were carried out at 4°C. The protein concentrations of the sEVs were measured using the bicinchoninic acid (BCA) assays (Beyotime). For the identification of sEVs, transmission electron microscopy (TEM) (HITACHI, Tokyo, Japan) was used to detect their morphology. Nanoparticle tracking analysis (NTA) was conducted using ZetaView (Particle Metrix, Meerbusch, Germany) to assess the size distribution of sEVs. Specific molecular markers of EVs, including TSG101, CD9, CD63, and CD81, were analyzed by Western blotting (WB).

Macrophage-Derived sEVs Uptake Assays

NPCs were isolated from the lumbar NP tissues of Sprague-Dawley (SD) rats as previously described.[6] Briefly, MΦ-sEVs were stained with 2 μM PKH26 red dye (Maokangbio, Shanghai, China) for 1 min. Then, the NPCs were treated with 40 μg/mL PKH26-labeled sEVs for 8 h and fixed with 4% paraformaldehyde (PFA) for 15 min. The cell cytoskeleton was labeled with FITC-conjugated phalloidin (Solarbio, Beijing, China), and cell nuclei were stained with DAPI. The NPCs were observed with confocal microscopy (Olympus, Tokyo, Japan).

Treatment of Bone Marrow-Derived Macrophages and Nucleus Pulposus Cells

NPCs were incubated with LPS+IFNγ-MΦ-CM, IL-4-MΦ-CM, 40 μg/mL LPS+IFNγ-MΦ-sEVs, or 40 μg/mL IL-4-MΦ-sEVs for 36 h. NPCs were detected by senescence-associated β-galactosidase (SA-β-Gal) staining, cell counting kit-8 (CCK-8), WB, and PCR analyses. The detailed methods of WB and PCR were described in the Supplementary Information 1. The antibodies and primer sequences used in this study are listed in Tables S1 and S2, respectively. The concentrations of inflammatory factors in the cell culture supernatant were measured by cytometric bead array (CBA). Transfection with miRNA mimics or inhibitors was conducted to regulate the miRNA levels in NPCs. The LIN28A inhibitor C1632 (Cayman, Ann Arbor, MI, USA) or siRNAs were used to evaluate the role of LIN28A in NPC senescence.

After removing the cell debris, the cell culture supernatant of IL-4-treated BMDMs was defined as IL-4-MΦ-CM. After ultracentrifugation, the cell culture supernatant was defined as the EV-free IL-4-MΦ-CM. Components in EV-free IL-4-MΦ-CM were analyzed by protein mass spectrometry (MS). Treatment of 10 μM GW4869 (Selleck, Houston, TX, USA) for 24 h was used to block the release of EVs from the BMDMs. After an additional 24 h culture in serum-free medium, the medium was harvested and designated as GW-IL-4-MΦ-CM. NPCs were treated with IL-4-MΦ-CM, EV-free IL-4-MΦ-CM, and GW-IL-4-MΦ-CM in various cell viability impairment models, including serum deprivation for 48 h, 100 μM tert-butyl hydroperoxide (TBHP) (Sigma-Aldrich, St. Louis, MO) treatment for 6 h, and 20 ng/mL rat IL-1β (PeproTech) treatment for 48 h.

Senescence-Associated β-Galactosidase Staining

NPC senescence levels were examined by the SA-β-Gal Staining Kit (Beyotime). After the indicated treatments, the NPCs were fixed with the fixing solution at room temperature for 15 min. Then, the cells were washed twice with PBS and incubated with freshly prepared staining solution at 37°C for 12 h. Total and blue-colored cells were counted under a light microscope (Olympus), and the ratio of SA-β-Gal positive cells was calculated.

Cell Counting Kit 8 Assays

Cell viability was measured by the CCK-8 assays (Bimake, Houston, TX, USA). The NPCs were seeded in the 96-well culture plates at a density of 5×10^3 cells per well. Following the treatment, the culture medium was discarded. Then, 10 μL CCK-8 reagent and 100 μL DMEM/F-12 medium were added to each well. After the incubation in the dark for 2 h at 37 °C, the absorbance at the wavelength of 450 nm (A450) was measured using a microplate reader (PerkinElmer).

Cytometric Bead Arrays

CBA was conducted to measure the concentrations of IL-1α, IL-1β, IL-6, tumor necrosis factor (TNF)-α and chemokine C-C motif ligand 2 (CCL2) in the cell culture supernatant using a LEGENDplex™ Rat Inflammation Panel (BioLegend, San Diego, CA). The reaction system, which is composed of 25 μL standard product or cell culture supernatant, 25 μL mixed beads, and 25 μL assay buffer, was incubated in the dark for 2 h at room temperature. After being washed with washing buffer, the beads were incubated with 25 μL detection antibody for 2 h and 25 μL SA-PE for 1 h. The fluorescence intensity of the beads was detected by FCM and analyzed using the LEGENDplex™ QOGNIT Software.

The in vivo Effects of Macrophage-Derived sEVs on Rat IVD Tissues

Animal experiments were approved by the Medical Ethics Committee of Tongji Medical College, Huazhong University of Science and Technology. The ARRIVE guidelines (Animal Research: Reporting of In Vivo Experiments) were followed by the current research.[21] Twenty-four two-month-old male SD rats were randomly divided into four groups (n = 6). After anesthesia with pentobarbital, Co7/8 IVD tissues were administrated with different treatments: sham group without injection, PBS group injected with 2 μL PBS, LPS+IFNγ-MΦ-sEVs group injected with 2 μL 100 μg/mL LPS +IFNγ-MΦ-sEVs in PBS, and IL-4-MΦ-sEVs group injected with 2 μL 100 μg/mL IL-4-MΦ-sEVs in PBS. Injection treatments were conducted every ten days for one month using a 33-gauge needle (Hamilton, Bonaduz, Switzerland).

After anesthesia, the rats were placed under an X-ray machine with their tails laid straight on the platform. Disc height was measured, and the disc height index (DHI) was calculated according to previous methods.[22] Magnetic resonance imaging (MRI) of coccygeal IVD tissues was performed using a 3-T scanner (PHILIPS), and the Pfirrmann Grade of T2-weighted MRI was analyzed.[23] The rats were euthanized by cervical dislocation after anesthesia. The methods of histological staining were detailedly stated in the Supplementary Information 1. Radiological and histological evaluations were performed by a researcher who was blinded to the grouping.

PANDORA Sequencing and Target Prediction

Small non-coding RNA sequencing of MΦ-sEVs was conducted using the panoramic RNA display by overcoming RNA modification aborted sequencing (PANDORA-seq) method.[24] Putative target genes of miRNAs were predicted by the miRDB (http://www.mirdb.org/), TargetScan (https://www.targetscan.org/vert_72/), and miRWalk (http://mirwalk.umm.uni-heidelberg.de/) databases.

Transfection of miRNA Mimic, miRNA Inhibitor, or siRNA

NPCs were transfected with 50 nM miRNA mimic, 100 nM miRNA inhibitor, 50 nM siRNA, or corresponding negative control (NC) RNA. Transfection was performed utilizing Lipofectamine 3000 reagent (Thermo Fisher Scientific, Waltham, MA, USA) following the manufacturer's instructions. The transfection efficacy was measured by PCR after 48 h. The siRNA sequences for *Lin28a* are shown in Table S3.

Luciferase Reporter Assays

The dual-luciferase vectors were constructed by cloning the wild-type (WT) or mutant (MUT) 3'-UTR sequence of *Lin28a* into the psiCHECK2 vector (Promega, Madison, WI, USA). To evaluate the direct binding between rno-let-7i-5p and *Lin28a* 3'-UTR, HEK293T cells were seeded in the 96-well plates at a density of 2×10^4 cells per well and transfected with the dual-luciferase vectors (psiCHECK2-*Lin28a*-WT or psiCHECK2-*Lin28a*-MUT) along with either NC mimic or rno-let-7i-5p mimic transfection. After 24 h, the HEK293T cells were collected and lysed. Firefly and Renilla luciferase activities were detected by the Dual-Glo Luciferase Assay System (Promega).

Statistical Analysis

For in vitro experiments of BMDMs and NPCs, rat primary cells in the five independent experiments were obtained from different donors. All continuous variables were presented as mean ± standard deviation, and statistical analyses were performed using the GraphPad Prism 7 Software (San Diego, CA, USA). Student's *t*-test (two groups) or one-way analysis of variance (ANOVA) followed by the least significant difference (LSD) test (three or more groups) was used to analyze statistical differences. For the MRI grading score and histological score, nonparametric test was used. $P < 0.05$ was regarded as statistical significance.

Results

LPS+IFNγ-MΦ-CM Stimulated Nucleus Pulposus Cell Inflammatory Response and ECM Catabolism

The phenotypes of the BMDMs were identified using FCM. The results showed that more than 90% cells were positive for CD11b/c and CD68. CD86 was highly expressed in LPS+IFNγ-MΦ, whereas CD206 was highly expressed in IL-4-MΦ (Figure 1A). RNA-seq also supported that LPS+IFNγ-MΦ expressed high levels of M1 macrophage markers (*Cd86, Ccr7*, etc.) and inflammatory factors (*Il1a, Il1b, Il6, Tnf*, etc.), while IL-4-MΦ expressed high levels of M2 macrophage markers (*Mrc1, Cd163*, etc.)[25] (Figure 1B, Figure S1 and Table S4). The levels of inflammatory factors in MΦ-CM were detected by CBA. The results indicated that LPS+IFNγ-MΦ secreted higher levels of IL-1α, IL-6, TNF-α, and CCL2 compared with IL-4-MΦ (Table S5).

The effects of MΦ-CM on NPC inflammatory response and ECM catabolism were measured by PCR, CBA, and WB. The results of PCR displayed that LPS+IFNγ-MΦ-CM stimulated higher expression levels of IL-1α, IL-1β, IL-6, CCL2, CCL5, TNF-α, matrix metalloproteinase (MMP)3, and MMP13 in NPCs, compared to the control group or IL-4-MΦ-CM group (Figure S2A). The concentrations of CCL2 and IL-6 in NPC culture supernatant were obviously elevated by LPS +IFNγ-MΦ-CM detected by CBA (Table S6). Moreover, multiple inflammatory pathways, including NOD-like receptor protein 3 (NLRP3), nuclear factor-κB (NF-κB) p65, and signal transducer and activator of transcription 3 (STAT3), were upregulated in NPCs treated with LPS+IFNγ-MΦ-CM (Figure S2B).

Identification and Cellular Uptake of Macrophage-Derived sEVs

MΦ-sEVs isolated by differential centrifugation were identified by size and morphology analysis. TEM displayed that the morphology of both LPS+IFNγ-MΦ-sEVs and IL-4-MΦ-sEVs were cup-shaped membrane structures (Figure 1C). NTA revealed that the diameters of LPS+IFNγ-MΦ-sEVs and IL-4-MΦ-sEVs were mainly distributed between 40 and 200 nm (Figure 1D). The expression of vesicle-specific markers, including TSG101, CD9, CD63, and CD81, was detected in both LPS+IFNγ-MΦ-sEVs and IL-4-MΦ-sEVs (Figure 1E). NPCs were treated with PKH26-labeled MΦ-sEVs to determine the uptake of sEVs. The fluorescence images demonstrated that both LPS+IFNγ-MΦ-sEVs and IL-4-MΦ-sEVs were internalized by NPCs (Figure 1F).

Macrophage-Derived sEVs Induced Nucleus Pulposus Cells Senescence

The effects of MΦ-sEVs on NPC senescence were assessed. SA-β-Gal staining and CCK-8 assays implied that both LPS +IFNγ-MΦ-sEVs and IL-4-MΦ-sEVs increased the ratio of senescent NPCs and impaired NPC viability compared with the control group (Figure 2A and B). SASP of senescent NPCs is featured with overactivated inflammatory response and

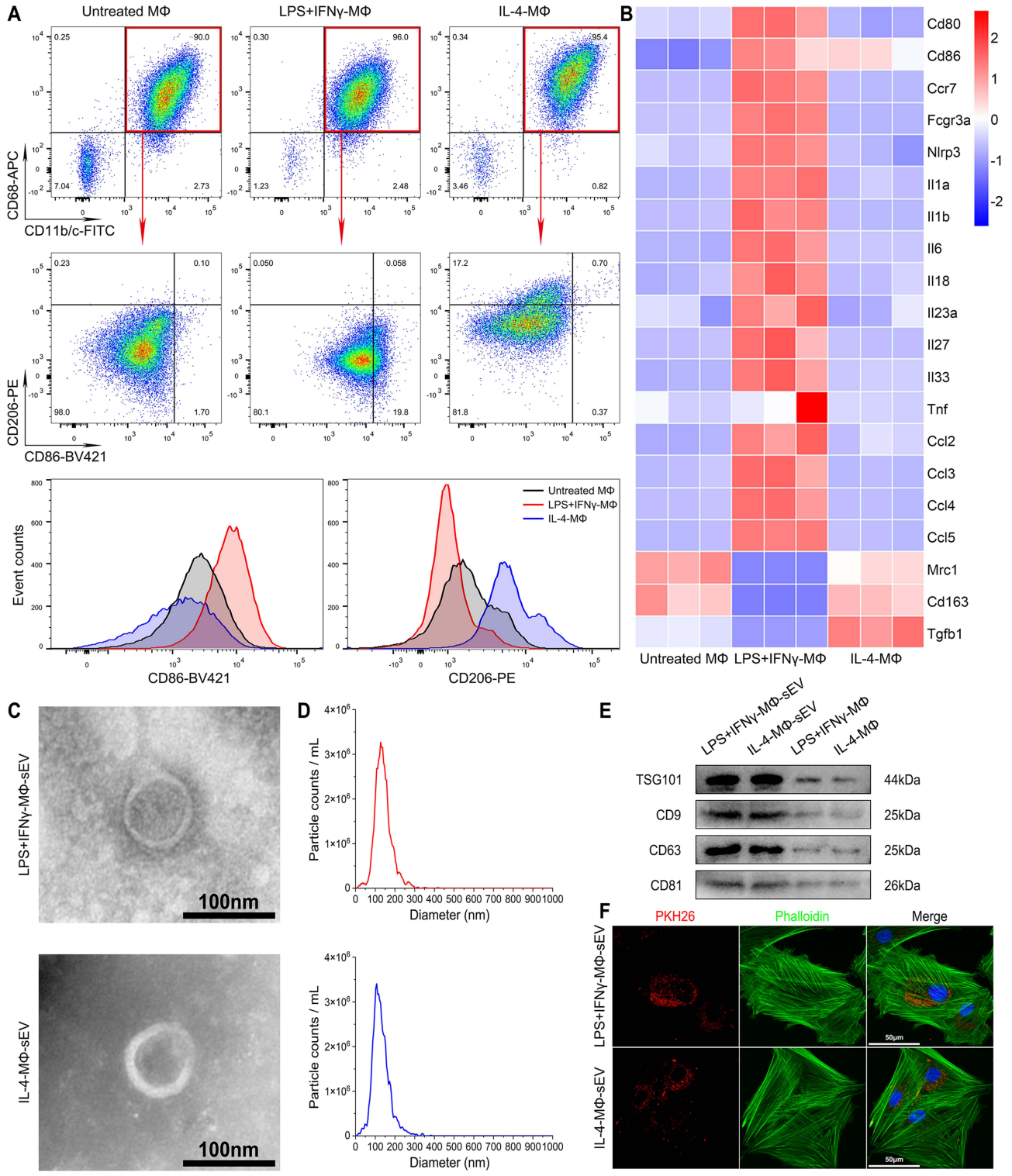

Figure 1 Identification of rat BMDMs and MΦ-sEV. (**A**) Representative FCM images of CD11b/c, CD68, CD86, and CD206 expression in rat BMDMs. (**B**) Heatmap of RNA-seq of rat BMDMs. Red represents high expression; blue represents low expression. (**C**) Representative TEM images showing the morphology and size of MΦ-sEVs. (**D**) The particle size distribution of MΦ-sEVs measured by NTA. (**E**) Representative WB graphs of TSG101, CD9, CD63, and CD81 in MΦ-sEVs and MΦ. (**F**) Typical fluorescence photomicrographs of the uptake of MΦ-sEVs by NPCs.

ECM catabolism.[18,19] The activation of NPC inflammatory response (*Il1a, Il6, Ccl2, Ccl5, Tnf*) and ECM catabolism (*Mmp3, Mmp13*), as well as the disruption of ECM anabolism (*Col2a1, Acan*), were detected in both LPS+IFNγ-MΦ-sEVs and IL-4-MΦ-sEVs groups (Figure 2C). CBA showed that the concentrations of CCL2 and IL-6 in NPC culture

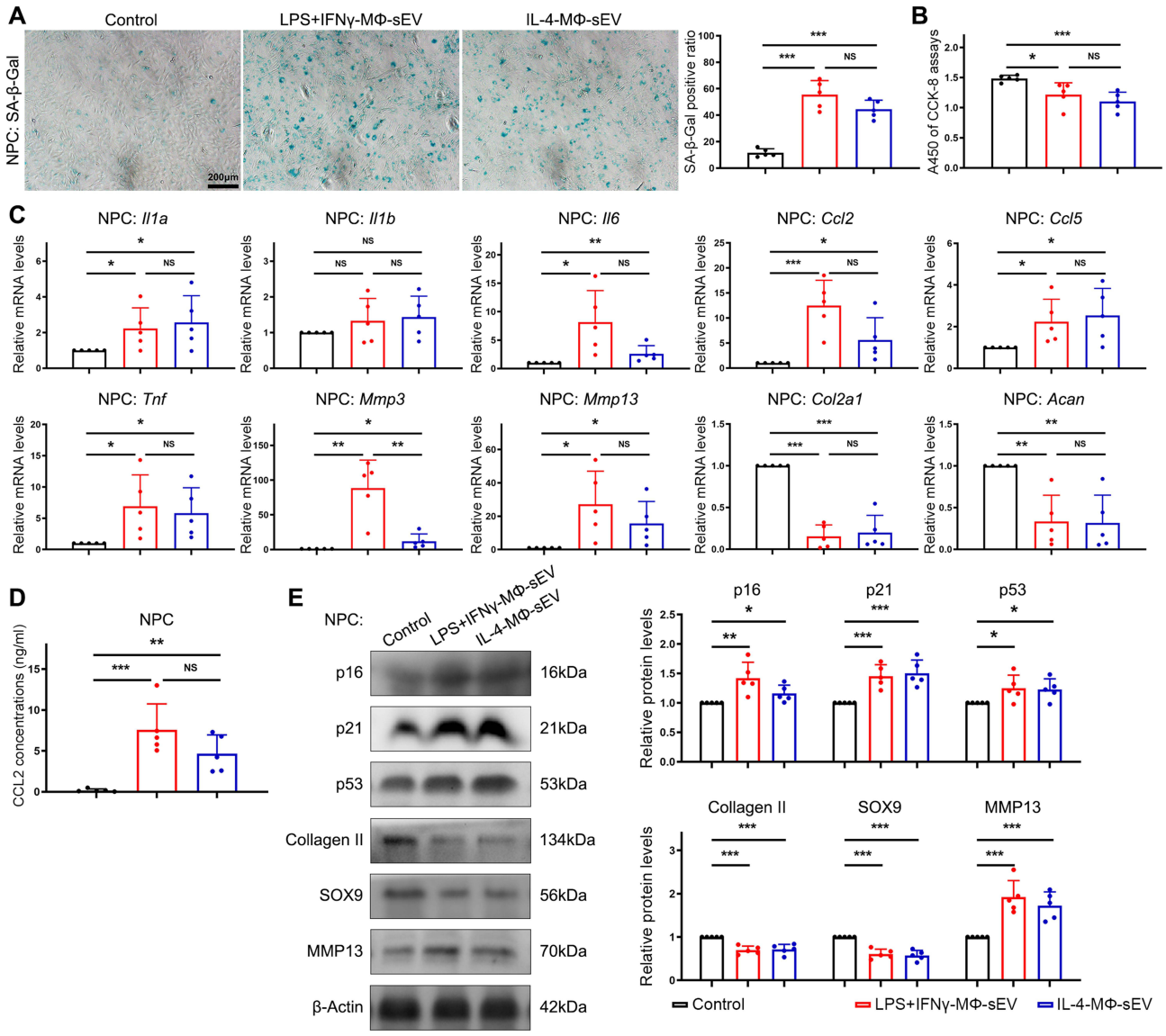

Figure 2 MΦ-sEVs induced NPC senescence. (**A**) Typical photomicrographs of senescent NPCs labeled with SA-β-Gal. (**B**) The viability of NPCs measured by CCK-8 assays. (**C**) The mRNA levels of *Il1a, Il1b, Il6, Ccl2, Ccl5, Tnf, Mmp3, Mmp13, Col2a1*, and *Acan* in NPCs. (**D**) The CCL2 concentrations in the CM of NPC detected by CBA. (**E**) Representative WB graphs of p16, p21, p53, Collagen II, SOX9, and MMP13 in NPCs. (NS: not significant, **P* < 0.05, ***P* < 0.01, ****P* < 0.001, n = 5).

supernatant were markedly elevated by LPS+IFNγ-MΦ-sEVs or IL-4-MΦ-sEVs treatment. The level of TNF-α was elevated in the LPS+IFNγ-MΦ-sEVs group (Figure 2D and Table S6). WB illustrated that the expression levels of p16, p21, p53, and MMP13 increased, while the expression levels of Collagen II and SOX9 decreased in NPCs after LPS +IFNγ-MΦ-sEVs or IL-4-MΦ-sEVs treatment (Figure 2D). Taken together, these results indicated that LPS+IFNγ-MΦ-sEVs or IL-4-MΦ-sEVs could induce NPC senescence and activate SASP.

Macrophage-Derived sEVs Exacerbated Intervertebral Disc Degeneration In vivo

MΦ-sEVs were injected into rat coccygeal IVD tissues, and the degree of degeneration was evaluated by radiological and histological analyses. X-ray images displayed decreased DHI in the LPS+IFNγ-MΦ-sEVs or IL-4-MΦ-sEVs group compared with the PBS group. On T2-weighted MRI, NP tissues of the sham and PBS groups showed homogeneous high signals and clear boundaries. In the LPS+IFNγ-MΦ-sEVs or IL-4-MΦ-sEVs group, the T2-weighted signal intensity of NP tissues was diminished to varying degrees, indicating an elevated Pfirrmann Grade (Figure 3A). HE and SOFG staining exhibited disorganized NP matrix structure and blurred boundary between NP and annulus fibrosus (AF) in the

https://doi.org/10.2147/IJN.S482646

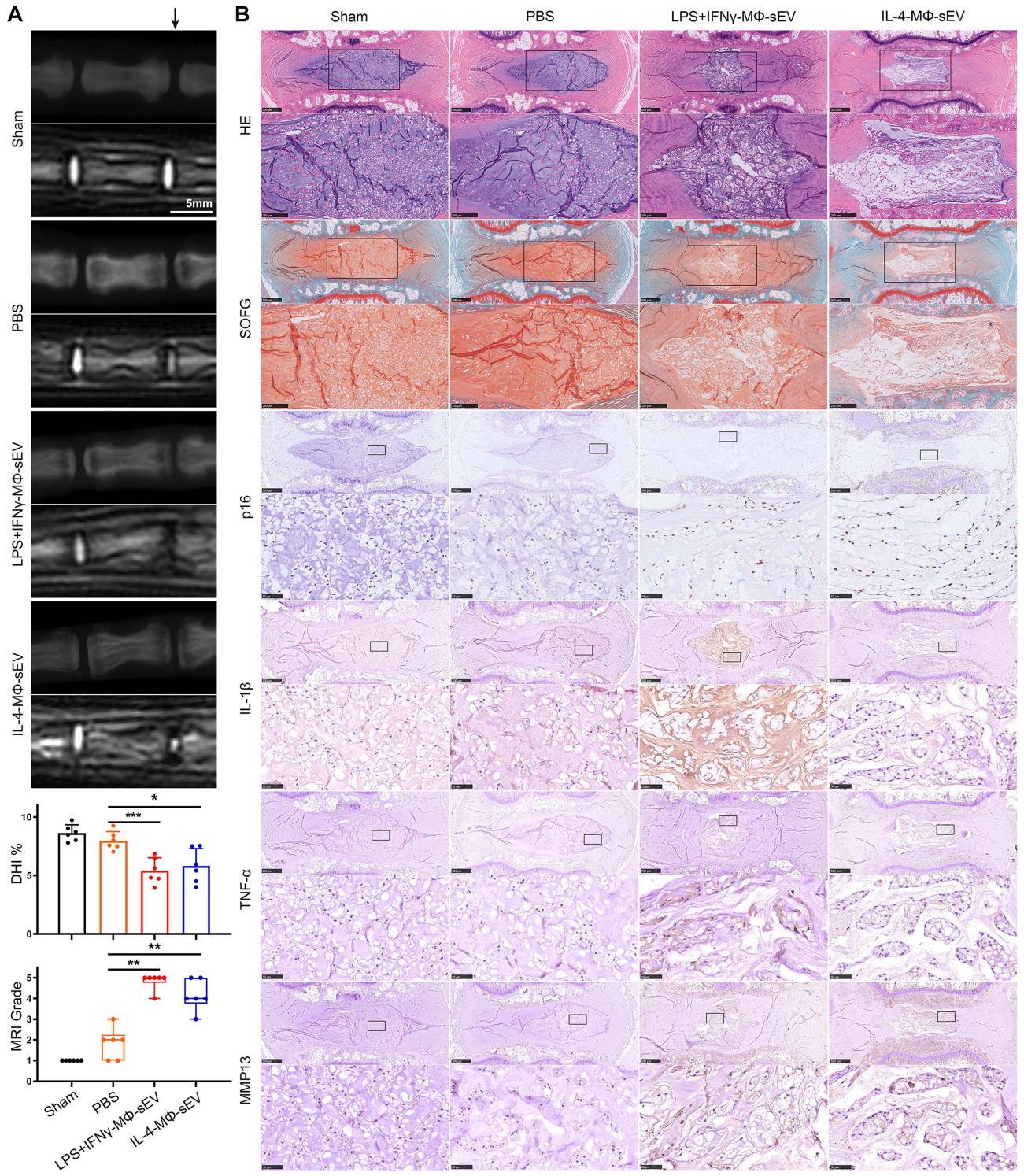

Figure 3 MΦ-sEVs exacerbated IVDD in vivo. (**A**) Representative X-ray and MRI images of rat coccygeal IVD tissues injected with MΦ-sEVs. (**B**) HE, SOFG, and IHC staining for p16, IL-1β, TNF-α, and MMP13 in rat coccygeal IVD tissues injected with MΦ-sEVs. (NS: not significant, *$P < 0.05$, **$P < 0.01$, ***$P < 0.001$, n = 6).

LPS+IFNγ-MΦ-sEVs or IL-4-MΦ-sEVs group. Histological grading was performed as previously reported, and the scores were markedly increased by MΦ-sEVs treatment[26] (Figure 3B and Figure S3A). Moreover, LPS+IFNγ-MΦ-sEVs or IL-4-MΦ-sEVs upregulated the proportion of p16-positive senescent cells, and the expression levels of inflammatory

factors IL-1β, TNF-α, and catabolic enzyme MMP13 in the NP region (Figure 3B and Figure S3B–E). Collectively, in vivo results indicated that both LPS+IFNγ-MΦ-sEVs and IL-4-MΦ-sEVs exacerbated IVDD.

PANDORA Sequencing of Macrophage-Derived sEVs

PANDORA sequencing was performed to estimate the miRNA levels in MΦ-sEVs. The results revealed that miR-3473, miR-27b-3p, let-7i-5p, miR-146a-5p, miR-191a-5p, miR-16-5p, miR-122-5p, miR-21-5p, miR-142-3p, and miR-29a-3p were highly expressed in LPS+IFNγ-MΦ-sEVs, whereas miR-27b-3p, miR-3473, miR-146a-5p, let-7i-5p, miR-16-5p, miR-21-5p, miR-142-3p, miR-191a-5p, miR-29a-3p, and miR-223-3p were highly expressed in IL-4-MΦ-sEVs (Figure 4A, Figure S4 and Table S7).

Overexpressing Let-7i-5p Induced Nucleus Pulposus Cells Senescence

Based on the sequencing results, the mimic transfection of six highly expressed miRNAs (miR-3473, miR-27b-3p, let-7i-5p, miR-146a-5p, miR-191a-5p, and miR-16-5p) into NPCs was conducted to screen the miRNAs with pro-senescence effects in MΦ-sEVs. The proportion of senescent NPCs was markedly higher in the let-7i-5p mimic group than in the NC mimic group (Figure 4B). PCR suggested that let-7i-5p exhibited stronger pro-inflammatory and pro-catabolic effects on NPCs. The levels of *Il1b, Il6, Ccl2*, and *Mmp3* were higher in the let-7i-5p mimic group than those in the NC mimic group (Figure 4C). In addition, let-7i-5p elevated the protein levels of p16, p21, p53, and MMP13 while decreasing Collagen II and SOX9 levels in NPCs (Figure 4D). Collectively, these data verified that let-7i-5p overexpression accelerates NPC senescence.

Lin28a is the Target of Let-7i-5p

The molecular mechanisms underlying the pro-senescence effects of let-7i-5p were further explored. MiRNAs usually bind to the 3'-UTR of the target mRNA to impede gene translation. Targets of rno-let-7i-5p were predicted using three databases (miRDB, TargetScan, and miRWalk). The Venn diagram detected four potential mRNA targets, which were *Adrb3, Arhgef15, Clp1*, and *Lin28a* (Figure 5A). RNA-binding protein LIN28A is widely involved in organismal growth and bioenergetic metabolism, possibly playing a regulatory role in cellular senescence.[27] Luciferase reporter assays verified that let-7i-5p could bind to the 3'-UTR of *Lin28a* mRNA, whereas mutation of the 3'-UTR restrained the binding process (Figure 5B). PCR and WB showed that treatment with LPS+IFNγ-MΦ-sEVs or IL-4-MΦ-sEVs increased the level of let-7i-5p and decreased the mRNA and protein levels of LIN28A in NPCs compared with the control group (Figure 5C–E). Moreover, overexpression of let-7i-5p by mimic transfection reduced LIN28A expression in NPCs (Figure 5F–H).

Macrophage-Derived sEVs or Aging Decreased LIN28A Expression in Nucleus Pulposus Tissues

The expression levels of LIN28A in rat NP tissues were examined by IHC staining. After LPS+IFNγ-MΦ-sEVs or IL-4-MΦ-sEVs treatment, the immune-reactivity of LIN28A declined in the rat coccygeal NP region (Figure 5I and Figure S3F). Moreover, the expression of LIN28A decreased prominently in both lumbar and coccygeal NP tissues with the increase in age, indicating the involvement of LIN28A in NP tissue aging (Figure 5J and K).

Inhibiting Let-7i-5p Ameliorated Nucleus Pulposus Cells Senescence Induced by Macrophage-Derived sEVs

The effects of the let-7i-5p inhibitor on MΦ-sEV-induced NPC senescence were further investigated. In LPS+IFNγ-MΦ-sEVs or IL-4-MΦ-sEVs treatment groups, let-7i-5p inhibitor transfection decreased SA-β-Gal positive ratios and reversed the LIN28A expression decline (Figure 6A–C). PCR showed that let-7i-5p inhibitor reduced the levels of *Il6, Ccl2, Mmp3*, and *Mmp13* in LPS+IFNγ-MΦ-sEVs groups, as well as the levels of *Il6, Ccl2*, and *Ccl5* in IL-4-MΦ-sEVs groups (Figure 6B). WB also demonstrated that inhibiting let-7i-5p efficiently downregulated senescence-related proteins (Figure 6C).

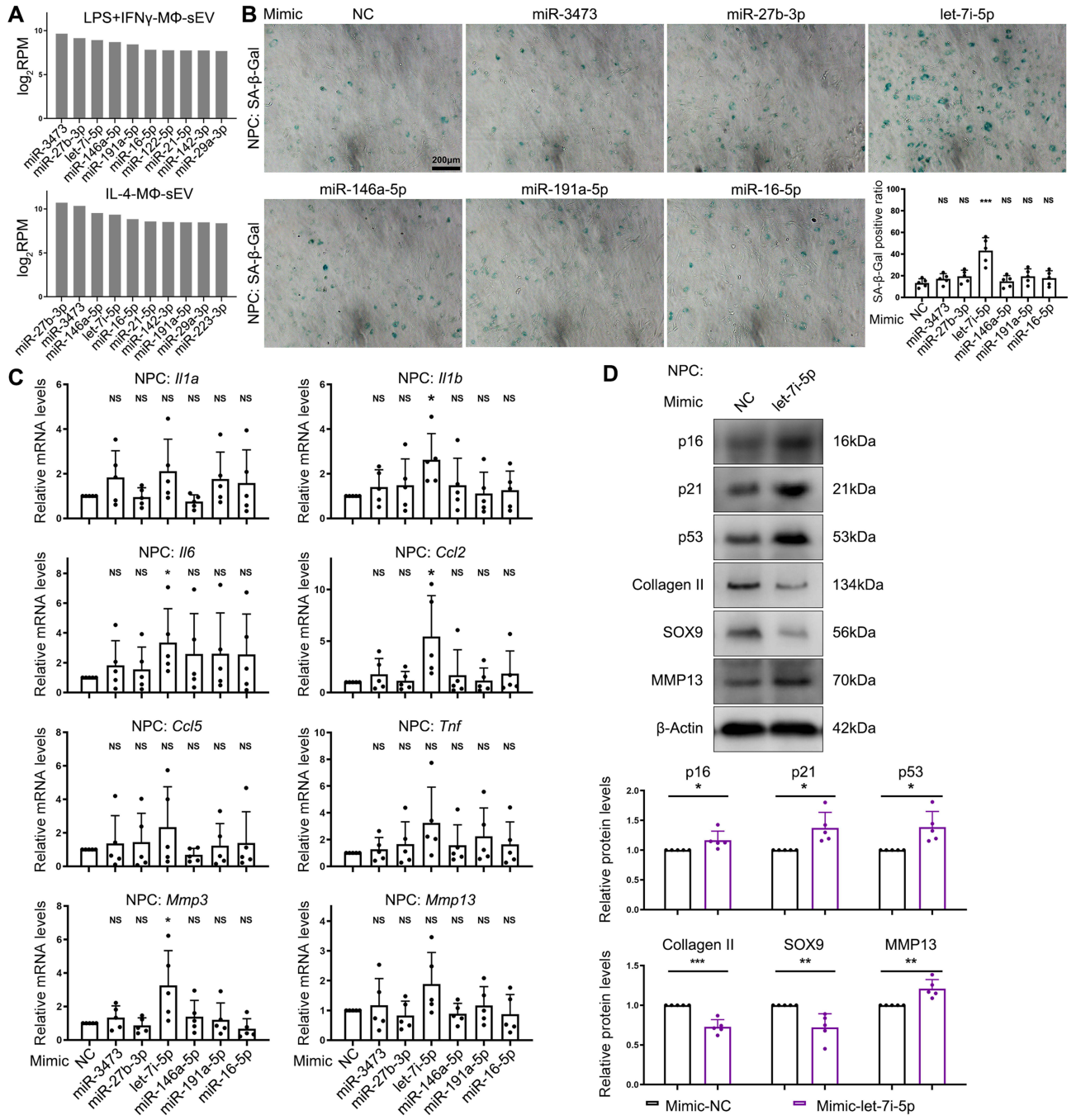

Figure 4 Let-7i-5p mimic induced NPC senescence. (**A**) PANDORA sequencing of MΦ-sEVs showing the miRNA levels. (**B**) Typical photomicrographs of senescent NPCs labeled with SA-β-Gal. (**C**) The mRNA levels of *Il1a, Il1b, Il6, Ccl2, Ccl5, Tnf, Mmp3*, and *Mmp13* in NPCs. (**D**) Representative WB graphs of p16, p21, p53, Collagen II, SOX9, and MMP13 in NPCs. (NS: not significant, *$P < 0.05$, **$P < 0.01$, ***$P < 0.001$, n = 5).

Inhibiting or Silencing LIN28A Induced Nucleus Pulposus Cells Senescence

LIN28A inhibitor C1632 or specific siRNAs were used to evaluate the role of LIN28A in NPC senescence. SA-β-Gal staining revealed that 100 μM C1632 dramatically amplified NPC senescence (Figure 7A). Additionally, CCK-8 assays showed that C1632 (10, 50, 100, 200, 500 μM) impaired NPC viability in a dose-dependent manner (Figure 7B). PCR and WB further supported the pro-senescence effects of C1632 (Figure 7C and D).

The transfection efficacy of the three *Lin28a* siRNAs was tested by PCR. Two siRNA sequences (si-*Lin28a*-1 and si-*Lin28a*-2), which obviously downregulated the mRNA level of *Lin28a*, were used in subsequent experiments

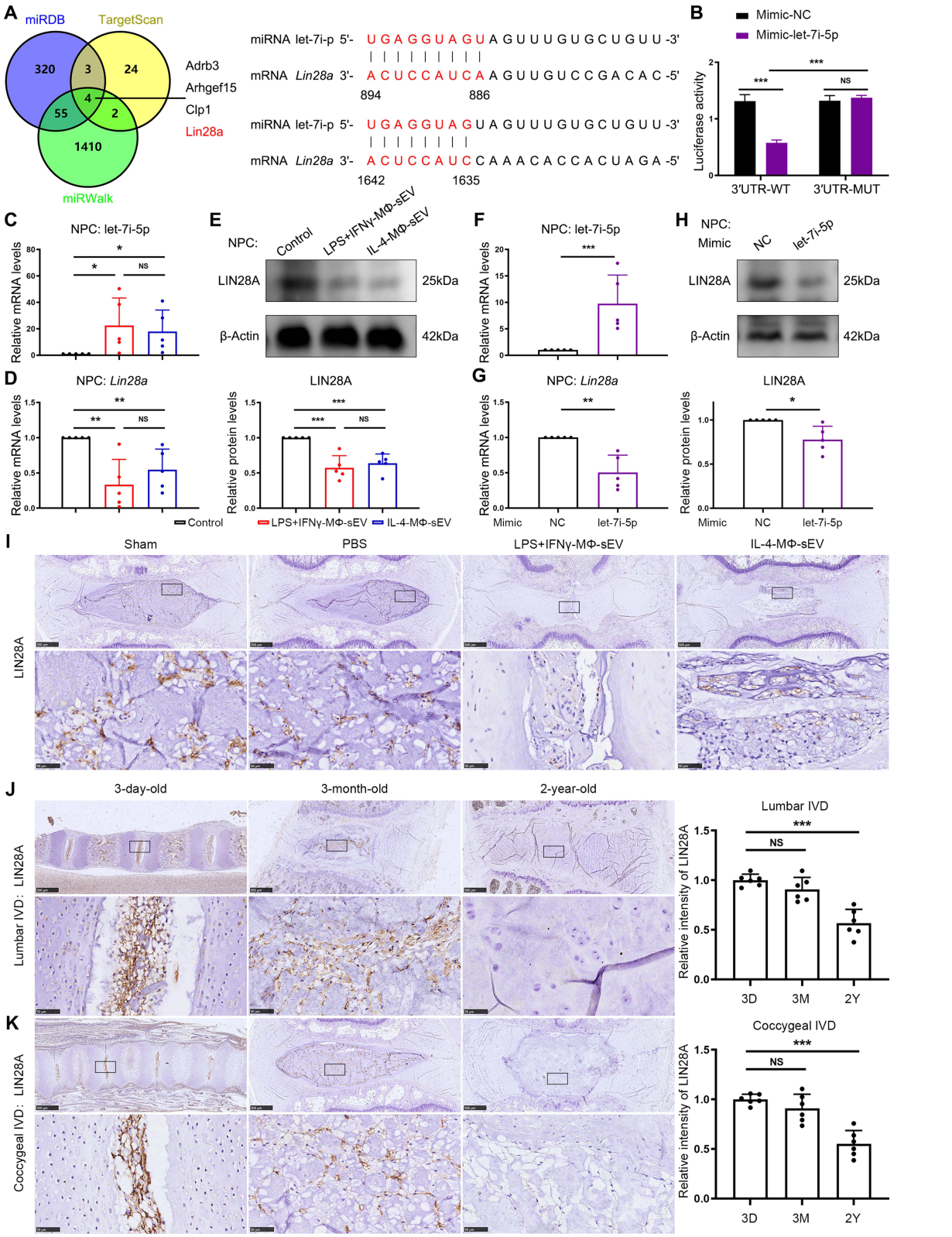

Figure 5 Let-7i-5p downregulated target gene *Lin28a*. (**A**) The potential target genes of let-7i-5p were predicted using the miRDB, TargetScan, and miRWalk databases. (**B**) The binding affinity of let-7i-5p with *Lin28a* 3'-UTR measured by dual-luciferase reporter assays. (**C**) The levels of miRNA let-7i-5p in NPCs. (**D**) The mRNA levels of *Lin28a* in NPCs. (**E**) Representative WB graphs of LIN28A in NPCs. (**F**) The levels of miRNA let-7i-5p in NPCs. (**G**) The mRNA levels of *Lin28a* in NPCs. (**H**) Representative WB graphs of LIN28A in NPCs. (**I**) IHC staining for LIN28A in rat coccygeal IVD tissues injected with MΦ-sEVs. (**J**) IHC staining for LIN28A in rat lumbar IVD tissues with different ages. (**K**) IHC staining for LIN28A in rat coccygeal IVD tissues with different ages. (NS: not significant, **P* < 0.05, ***P* < 0.01, ****P* < 0.001, n = 5 in B-H, n = 6 in I-K).

https://doi.org/10.2147/IJN.S482646

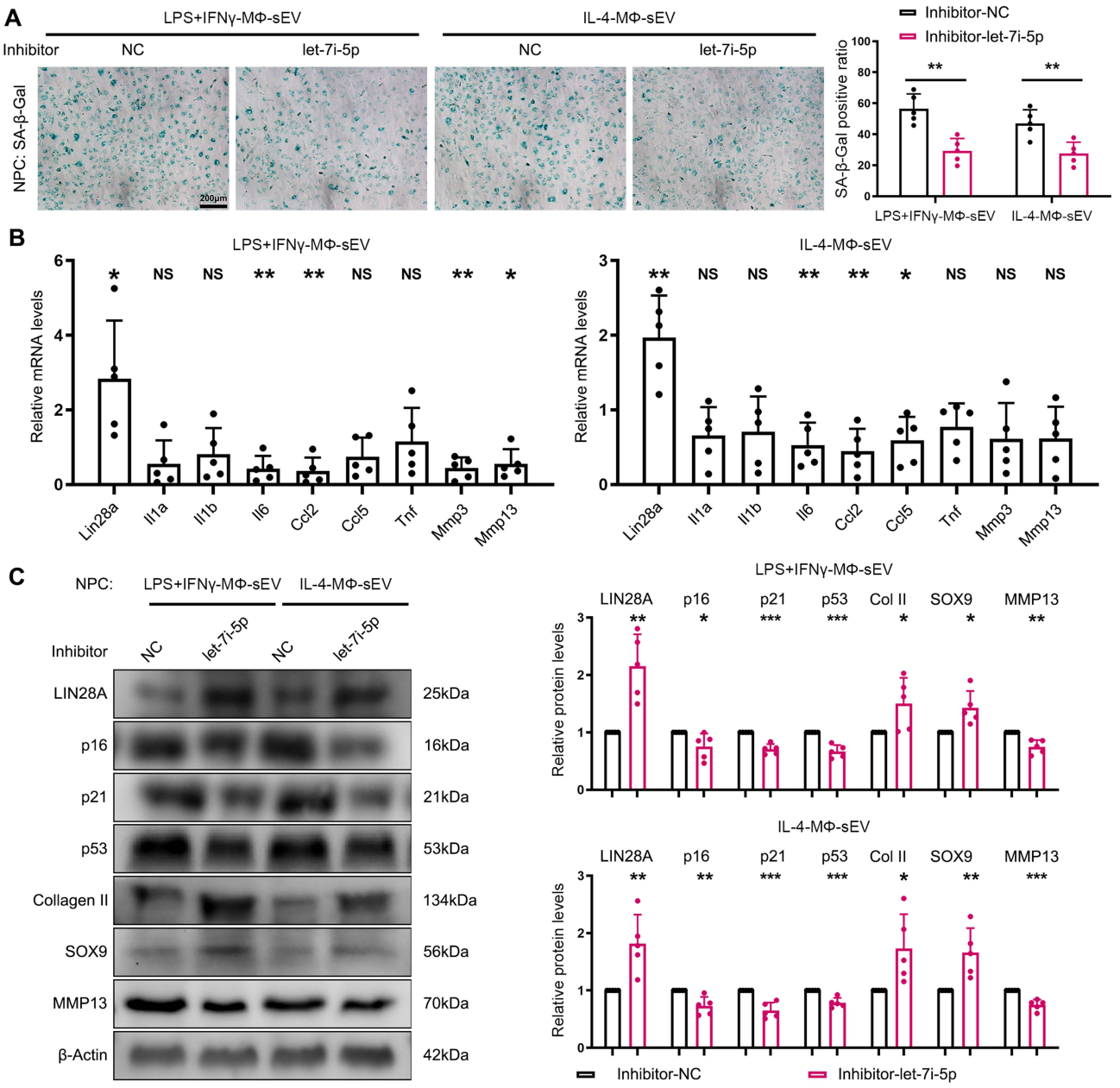

Figure 6 Let-7i-5p inhibitor ameliorated NPC senescence induced by MΦ-sEVs. (**A**) Typical photomicrographs of senescent NPCs labeled with SA-β-Gal. (**B**) The mRNA levels of *Lin28a, Il1a, Il1b, Il6, Ccl2, Ccl5, Tnf, Mmp3*, and *Mmp13* in NPCs. (**C**) Representative WB graphs of LIN28A, p16, p21, p53, Collagen II, SOX9, and MMP13 in NPCs. (NS: not significant, **P* < 0.05, ***P* < 0.01, ****P* < 0.001, n = 5).

(Figure 7E). In accordance with the LIN28A inhibitor C1632, silencing *Lin28a* by siRNA also increased senescent NPC ratio, activated SASP expression (*Il1a, Il1b, Il6, Ccl2, Ccl5, Tnf, Mmp3*, and *Mmp13*), and stimulated senescence pathways (p16, p21, and p53) (Figure 7F–H).

Removal of EVs Improved the Cytoprotective Effects of IL-4-MΦ-CM

The current section aimed to explore the cytoprotective effects of IL-4-MΦ-CM on NPCs and the underlying molecular mechanisms. IL-4-MΦs were treated with GW4869 to reduce sEVs release, as verified by NTA and WB (Figure S5A and B). The results of CCK-8 assays showed that EV-free IL-4-MΦ-CM and GW-IL-4-MΦ-CM mildly ameliorated NPC viability loss induced by serum deprivation treatment for 48 h, 100 μM TBHP treatment for 6 h, and 20 ng/mL IL-1β treatment for 48 h (Figure S5C).

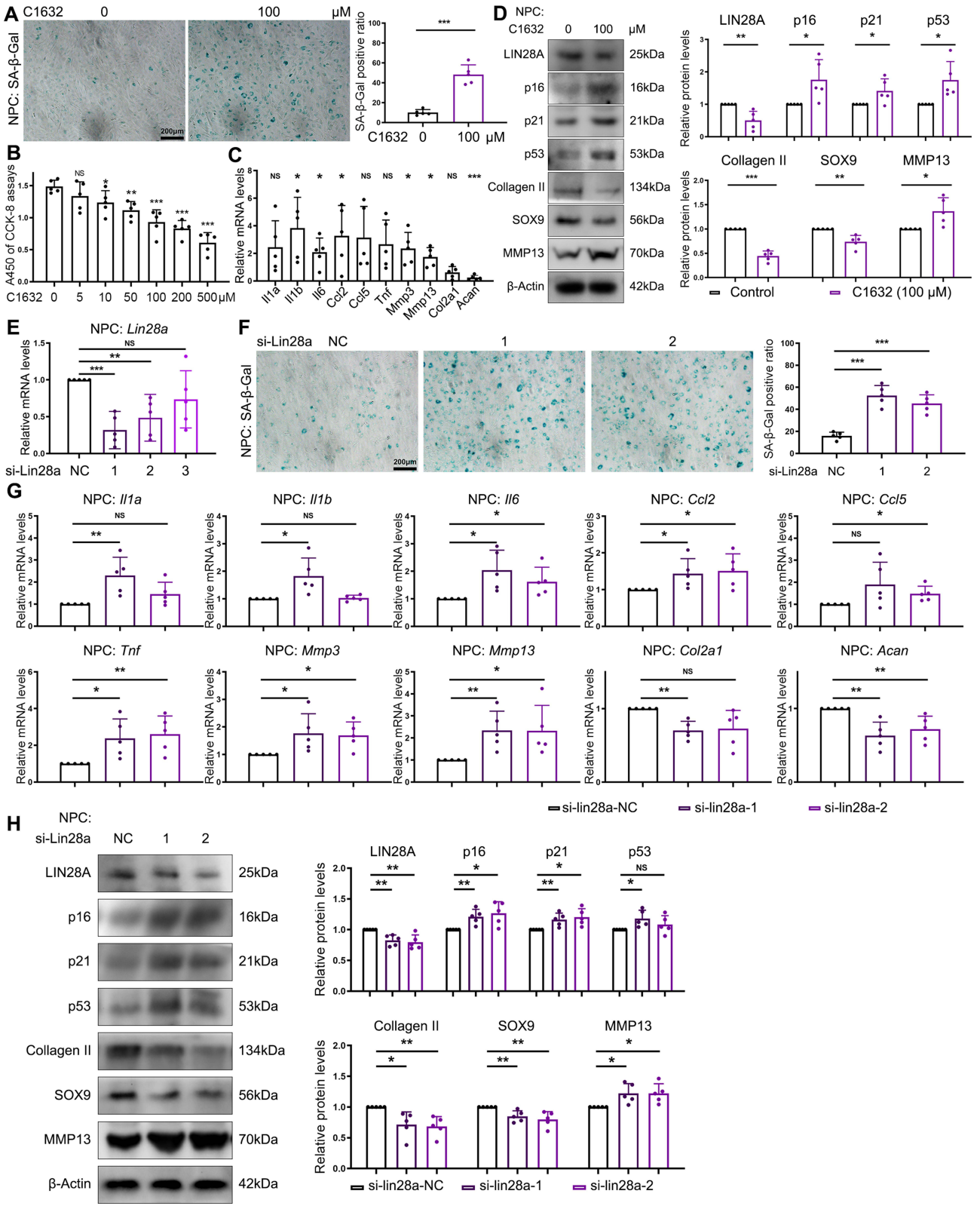

Figure 7 Inhibiting or silencing LIN28A induced NPC senescence. (**A**) Typical photomicrographs of senescent NPCs labeled with SA-β-Gal. (**B**) The viability of NPCs measured by CCK-8 assays. (**C**) The mRNA levels of *Il1a, Il1b, Il6, Ccl2, Ccl5, Tnf, Mmp3, Mmp13, Col2a1*, and *Acan* in NPCs. (**D**) Representative WB graphs of LIN28A, p16, p21, p53, Collagen II, SOX9, and MMP13 in NPCs. (**E**) The mRNA levels of *Lin28a* in NPCs. (**F**) Typical photomicrographs of senescent NPCs labeled with SA-β-Gal. (**G**) The mRNA levels of *Il1a, Il1b, Il6, Ccl2, Ccl5, Tnf, Mmp3, Mmp13, Col2a1*, and *Acan* in NPCs. (**H**) Representative WB graphs of LIN28A, p16, p21, p53, Collagen II, SOX9, and MMP13 in NPCs. (NS: not significant, **P* < 0.05, ***P* < 0.01, ****P* < 0.001, n = 5).

https://doi.org/10.2147/IJN.S482646

Protein profiling was performed to identify potential cytoprotective factors in EV-free IL-4-MΦ-CM. The results detected high intensities of the immunomodulators thymosin β4, thymosin β10, and prothymosin α (Table S8), which were previously reported to protect IVD cell viability.[28,29] RNA-seq and PCR further suggested that the expression levels of *Tmsb4x, Tmsb10*, and *Ptma* in IL-4-MΦ were higher than those in LPS+IFNγ-MΦ (Figure S5D and E).

Discussion

Cellular senescence dramatically damages the function of IVD cells and deteriorates the microenvironment of IVD tissues. Multiple adverse factors, including excessive mechanical stress, inflammation, oxidative stress, and nutritional deprivation, may lead to IVD cell senescence.[18,19] Anti-senescence therapies, including senolysis and senomorphics, are promising strategies for reversing the accumulation of senescent cells and maintaining the physiological structure and function of IVD tissues. Senolytic strategies that selectively eliminate senescent cells using transgenic technology or senolytic drugs can effectively relieve IVDD in animal models.[30,31] Senomorphics improves the properties of senescent cells by alleviating DNA damage, activating telomerase and autophagy, and relieving oxidative stress and inflammatory response. Therefore, it is essential to further explore the underlying mechanisms and treatment strategies for NPC senescence.

Cell senescence and macrophage infiltration are closely linked pathological processes. Senescent cardiac mesenchymal stem cells (MSCs) recruited macrophages by secreting the CCR2 ligands CCL2, CCL8, CXCL12, and CX3CL1. Pro-inflammatory macrophage activation further induced MSC senescence, forming a vicious circle of inflammation cascades.[32] Degenerated IVD tissues or cells can also recruit and activate inflammatory macrophages by releasing chemokines or exosomes.[4,33] On the other hand, inflammatory macrophages deteriorate the microenvironment and stimulate cellular senescence in the IVD tissues.[5,34] The crosstalk between pro-inflammatory macrophages and degenerative NPCs may form a vicious circle, consistently impairing NPC viability and biosynthesis.

MΦ-sEVs are widely involved in the communication processes between macrophages and other cells.[35] The exosomes from LPS-treated macrophages could induce NPC senescence and lead to IVDD via activating the NF-κB signaling.[36] Similarly, the development of OA was also accelerated by the EVs from LPS-treated macrophages.[10] Conversely, the exosomes from IL-10-treated macrophages could mitigate IVDD by carrying miR-124-3p.[37] Furthermore, the application of engineered nanoparticles based on IL-4-MΦ-sEVs was a promising anti-inflammatory strategy in the treatment of rheumatoid arthritis.[38] In contrast to other studies, our results found that both LPS+IFNγ-MΦ-sEVs and IL-4-MΦ-sEVs triggered senescence and activated the SASP of NPC in vitro and in vivo. Moreover, the PANDORA-seq revealed similar highly expressed miRNA profiles. In another non-coding RNA sequencing study on human macrophage-derived EVs, the relative abundance of miRNAs was higher in M1-EVs than in M2-EVs. hsa-let-7i-5p ranked as the first highest miRNA in M1-EVs, and the sixth highest miRNA in M2-EVs.[39] Similarity and diversity may coexist between the M1-EVs and M2-EVs. Therefore, it is necessary to further investigate the complexity and multifunctionality of MΦ-sEVs in different tissues.

Let-7 family miRNAs are highly expressed in various aging tissues and participate in the pathogenesis of age-related diseases, such as musculoskeletal degenerative diseases, neurodegenerative diseases, age-related eye diseases, etc.[40] Exosomal let-7i-5p exerted pro-inflammatory effects and aggravated PM2.5-associated asthma via activating the mitogen-activated protein kinase (MAPK) signaling pathway.[41] The mutually inhibitory feedback loop between let-7 and LIN28A has been implicated in the regulation of multiple biological processes, including stem cell function, cellular metabolism, and oncogenesis.[42] Let-7 miRNAs bind to the 3'-UTR of LIN28A and suppress LIN28A expression, while LIN28A blocks the maturation of let-7 miRNA precursors.[43] LIN28A plays an important role in cartilage development and regeneration. During articular cartilage (AC) development, LIN28A overexpression in cartilage progenitor cells increased AC thickness by activating the extracellular signal-regulated kinase (ERK) pathway.[44] LIN28A promoted the proliferation and anabolism of chondrocytes and attenuated catabolism, which was conducive to cartilage injury repair in mice. Moreover, LIN28A knockout in chondrocytes aggravated cartilage destruction in a mouse osteoarthritis model.[45] It was also reported that LIN28A mediated cartilage and bone regeneration by modulating glycolysis and oxidative phosphorylation (OxPhos).[27] In this study, PANDORA-seq revealed that both LPS+IFNγ-MΦ-sEVs and IL-4-MΦ-

sEVs contained high levels of let-7i-5p. Compared to other highly expressed miRNAs in sEVs, let-7i-5p could induce NPC senescence and activate SASP by downregulating LIN28A.

In contrast to IL-4-MΦ-sEVs, EVs-free IL-4-MΦ-CM protected NPC in several cell viability impairment models. Protein profiling was performed to uncover the underlying mechanisms. The results showed high levels of thymosin and prothymosin, which were crucial immunomodulators with anti-inflammatory and tissue-repairing effects. Overexpression of thymosin β4 by adeno-associated virus transfection inhibited NPC apoptosis and senescence and promoted NPC proliferation.[28] The anti-apoptosis effects on AF cells in vitro and the pro-healing effects on cardiac wounds of thymosin β4 were also reported previously.[29,46] Prothymosin α could protect endothelial cells and retinal cells from adverse stimuli.[47,48] Furthermore, the combination of thymosin β4 and prothymosin α enhanced cardiomyocyte proliferation, thereby promoting cardiac regeneration.[49] The current study demonstrated that IL-4-MΦ secreted higher levels of cytoprotective and immunoregulatory peptides thymosin β4, thymosin β10, and prothymosin α than untreated MΦ and LPS+IFNγ-MΦ. Considering the pro-inflammatory and pro-catabolic effects of M1 macrophages, it is assumed that the repolarization of macrophages from M1-type to M2-type is potentially conducive to improving the IVD microenvironment and preventing further degeneration.[50]

This study had several limitations. First, the contents of MΦ-sEVs are complex. Therefore, it was arbitrary to attribute the overall effects of sEVs to a single miRNA. Various inflammatory and chemotactic factors, such as TNF-α, CCL3, CCL22, CXCL2, and CXCL10, were also detected in the exosomes from LPS-treated RAW264.7 macrophages.[51] Second, the quantity and content changes of MΦ-sEVs during IVDD were difficult to analyze. In vitro experiments might not completely simulate the pathological processes in vivo.

Conclusion

Both LPS+IFNγ-MΦ-sEVs and IL-4-MΦ-sEVs induced NPC senescence by delivering miRNA let-7i-5p to inhibit LIN28A. The effects of MΦ-sEVs should not be ignored in the pathogenesis of IVDD and targeted therapeutic strategies require further investigations.

Acknowledgments

We would like to thank the Experimental Animal Center of Tongji Medical College, Huazhong University of Science and Technology, for their help with the animal care and study. We would like to thank Guangzhou Epibiotek Co. for sequencing data analysis and visualization.

Funding

This work was supported by the National Natural Science Foundation of China 82402875 (S.Z.), 82372472 (S.C.), and 82472513 (X.L.); the Henan Provincial Science and Technology Research and Development Plan Joint Fund Cultivation Project 222301420048 (S.C.); the Key Scientific Research Project Plan of Colleges and Universities in Henan Province 24A320016 (S.C.).

Disclosure

The authors report no conflicts of interest in this work.

References

1. Risbud MV, Shapiro IM. Role of cytokines in intervertebral disc degeneration: pain and disc content. *Nat Rev Rheumatol*. 2014;10(1):44–56. doi:10.1038/nrrheum.2013.160
2. Zhang S, Liu W, Chen S, et al. Extracellular matrix in intervertebral disc: basic and translational implications. *Cell Tissue Res*. 2022;390(1):1–22. doi:10.1007/s00441-022-03662-5
3. Zhang S, Wang P, Hu B, et al. HSP90 Inhibitor 17-AAG Attenuates Nucleus Pulposus Inflammation and Catabolism Induced by M1-Polarized Macrophages. *Front Cell Dev Biol*. 2021;9:796974. doi:10.3389/fcell.2021.796974
4. Tian S, Chen X, Wu W, et al. Nucleus pulposus cells regulate macrophages in degenerated intervertebral discs via the integrated stress response-mediated CCL2/7-CCR2 signaling pathway. *Exp Mol Med*. 2024;56(2):408–421. doi:10.1038/s12276-024-01168-4
5. Wang P, Zhang S, Liu W, et al. Bardoxolone methyl breaks the vicious cycle between M1 macrophages and senescent nucleus pulposus cells through the Nrf2/STING/NF-κB pathway. *Int Immunopharmacol*. 2024;127:111262. doi:10.1016/j.intimp.2023.111262

6. Zhang S, Wang P, Hu B, et al. Inhibiting Heat Shock Protein 90 Attenuates Nucleus Pulposus Fibrosis and Pathologic Angiogenesis Induced by Macrophages via Down-Regulating Cell Migration-Inducing Protein. *Am J Pathol*. 2023;193(7):960–976. doi:10.1016/j.ajpath.2023.03.014
7. Li XC, Luo SJ, Fan W, Zhou TL, Huang CM, Wang MS. M2 macrophage-conditioned medium inhibits intervertebral disc degeneration in a tumor necrosis factor-α-rich environment. *J Orthop Res*. 2022;40(11):2488–2501. doi:10.1002/jor.25292
8. Li XC, Luo SJ, Fan W, et al. Macrophage polarization regulates intervertebral disc degeneration by modulating cell proliferation, inflammation mediator secretion, and extracellular matrix metabolism. *Front Immunol*. 2022;13:922173. doi:10.3389/fimmu.2022.922173
9. Kalluri R, LeBleu VS. The biology, function, and biomedical applications of exosomes. *Science*. 2020;367(6478):eaau6977. doi:10.1126/science.aau6977
10. Ebata T, Terkawi MA, Kitahara K, et al. Noncanonical Pyroptosis Triggered by Macrophage-Derived Extracellular Vesicles in Chondrocytes Leading to Cartilage Catabolism in Osteoarthritis. *Arthritis Rheumatol*. 2023;75(8):1358–1369. doi:10.1002/art.42505
11. Lim Y, Kim HY, Han D, Choi B-K. Proteome and immune responses of extracellular vesicles derived from macrophages infected with the periodontal pathogen Tannerella forsythia. *J Extracell Vesicles*. 2023;12(12):e12381. doi:10.1002/jev2.12381
12. Mori MA, Ludwig RG, Garcia-Martin R, Brandão BB, Kahn CR. Extracellular miRNAs: from Biomarkers to Mediators of Physiology and Disease. *Cell Metab*. 2019;30(4):656–673. doi:10.1016/j.cmet.2019.07.011
13. O'Brien K, Breyne K, Ughetto S, Laurent LC, Breakefield XO. RNA delivery by extracellular vesicles in mammalian cells and its applications. *Nat Rev mol Cell Biol*. 2020;21(10):585–606. doi:10.1038/s41580-020-0251-y
14. Fabian MR, Sonenberg N, Filipowicz W. Regulation of mRNA translation and stability by microRNAs. *Annu Rev Biochem*. 2010;79(1):351–379. doi:10.1146/annurev-biochem-060308-103103
15. Jonas S, Izaurralde E. Towards a molecular understanding of microRNA-mediated gene silencing. *Nat Rev Genet*. 2015;16(7):421–433. doi:10.1038/nrg3965
16. Cazzanelli P, Wuertz-Kozak K. MicroRNAs in Intervertebral Disc Degeneration, Apoptosis, Inflammation, and Mechanobiology. *Int J mol Sci*. 2020;21(10):3601. doi:10.3390/ijms21103601
17. López-Otín C, Blasco MA, Partridge L, Serrano M, Kroemer G. Hallmarks of aging: an expanding universe. *Cell*. 2023;186(2):243–278. doi:10.1016/j.cell.2022.11.001
18. Wang F, Cai F, Shi R, Wang XH, Wu XT. Aging and age related stresses: a senescence mechanism of intervertebral disc degeneration. *Osteoarthritis Cartilage*. 2016;24(3):398–408. doi:10.1016/j.joca.2015.09.019
19. Silwal P, Nguyen-Thai AM, Mohammad HA, et al. Cellular Senescence in Intervertebral Disc Aging and Degeneration: molecular Mechanisms and Potential Therapeutic Opportunities. *Biomolecules*. 2023;13(4):686. doi:10.3390/biom13040686
20. Théry C, Amigorena S, Raposo G, Clayton A. Isolation and characterization of exosomes from cell culture supernatants and biological fluids. *Curr Protoc Cell Biol*. 2006;3:322. doi:10.1002/0471143030.cb0322s30
21. du Sert N P, Hurst V, Ahluwalia A, et al. The ARRIVE guidelines 2.0: updated guidelines for reporting animal research. *PLoS Biol*. 2020;18(7):e3000410. doi:10.1371/journal.pbio.3000410
22. Han B, Zhu K, Li FC, et al. A simple disc degeneration model induced by percutaneous needle puncture in the rat tail. *Spine*. 2008;33(18):1925–1934. doi:10.1097/BRS.0b013e31817c64a9
23. Pfirrmann CW, Metzdorf A, Zanetti M, Hodler J, Boos N. Magnetic resonance classification of lumbar intervertebral disc degeneration. *Spine*. 2001;26(17):1873–1878. doi:10.1097/00007632-200109010-00011
24. Shi J, Zhang Y, Tan D, et al. PANDORA-seq expands the repertoire of regulatory small RNAs by overcoming RNA modifications. *Nat Cell Biol*. 2021;23(4):424–436. doi:10.1038/s41556-021-00652-7
25. Murray PJ. Macrophage Polarization. *Annu Rev Physiol*. 2017;79(1):541–566. doi:10.1146/annurev-physiol-022516-034339
26. Rutges JP, Duit RA, Kummer JA, et al. A validated new histological classification for intervertebral disc degeneration. *Osteoarthritis Cartilage*. 2013;21(12):2039–2047. doi:10.1016/j.joca.2013.10.001
27. Shyh-Chang N, Zhu H, Yvanka de Soysa T, et al. Lin28 enhances tissue repair by reprogramming cellular metabolism. *Cell*. 2013;155(4):778–792. doi:10.1016/j.cell.2013.09.059
28. Wang YY, Zhu QS, Wang YW, Yin RF. Thymosin Beta-4 Recombinant Adeno-associated Virus Enhances Human Nucleus Pulposus Cell Proliferation and Reduces Cell Apoptosis and Senescence. *Chin Med J*. 2015;128(11):1529–1535. doi:10.4103/0366-6999.157686
29. Tapp H, Deepe R, Ingram JA, et al. Exogenous thymosin beta4 prevents apoptosis in human intervertebral annulus cells in vitro. *Biotech Histochem*. 2009;84(6):287–294. doi:10.3109/10520290903116884
30. Che H, Li J, Li Y, et al. p16 deficiency attenuates intervertebral disc degeneration by adjusting oxidative stress and nucleus pulposus cell cycle. *Elife*. 2020;9:e52570. doi:10.7554/eLife.52570
31. Novais EJ, Tran VA, Johnston SN, et al. Long-term treatment with senolytic drugs Dasatinib and Quercetin ameliorates age-dependent intervertebral disc degeneration in mice. *Nat Commun*. 2021;12(1):5213. doi:10.1038/s41467-021-25453-2
32. Martini H, Iacovoni JS, Maggiorani D, et al. Aging induces cardiac mesenchymal stromal cell senescence and promotes endothelial cell fate of the CD90 + subset. *Aging Cell*. 2019;18(5):e13015. doi:10.1111/acel.13015
33. Zhao X, Sun Z, Xu B, et al. Degenerated nucleus pulposus cells derived exosome carrying miR-27a-3p aggravates intervertebral disc degeneration by inducing M1 polarization of macrophages. *J Nanobiotechnology*. 2023;21(1):317. doi:10.1186/s12951-023-02075-y
34. Song C, Zhou Y, Cheng K, et al. Cellular senescence - Molecular mechanisms of intervertebral disc degeneration from an immune perspective. *Biomed Pharmacother*. 2023;162:114711. doi:10.1016/j.biopha.2023.114711
35. Wang Y, Zhao M, Liu S, et al. Macrophage-derived extracellular vesicles: diverse mediators of pathology and therapeutics in multiple diseases. *Cell Death Dis*. 2020;11(10):924. doi:10.1038/s41419-020-03127-z
36. Fan C, Wang W, Yu Z, et al. M1 macrophage-derived exosomes promote intervertebral disc degeneration by enhancing nucleus pulposus cell senescence through LCN2/NF-κB signaling axis. *J Nanobiotechnology*. 2024;22(1):301. doi:10.1186/s12951-024-02556-8
37. Liu Y, Xue M, Han Y, et al. Exosomes from M2c macrophages alleviate intervertebral disc degeneration by promoting synthesis of the extracellular matrix via MiR-124/CILP/TGF-β. *Bioeng Transl Med*. 2023;8(6):e10500. doi:10.1002/btm2.10500
38. Li H, Feng Y, Zheng X, et al. M2-type exosomes nanoparticles for rheumatoid arthritis therapy via macrophage re-polarization. *J Control Release*. 2022;341:16–30. doi:10.1016/j.jconrel.2021.11.019

39. Pantazi P, Clements T, Venø M, Abrahams VM, Holder B. Distinct non-coding RNA cargo of extracellular vesicles from M1 and M2 human primary macrophages. *J Extracell Vesicles*. 2022;11(12):e12293. doi:10.1002/jev2.12293
40. Wang Y, Zhao J, Chen S, et al. Let-7 as a Promising Target in Aging and Aging-Related Diseases: a Promise or a Pledge. *Biomolecules*. 2022;12 (8):1070. doi:10.3390/biom12081070
41. Zheng R, Du M, Tian M, et al. Fine Particulate Matter Induces Childhood Asthma Attacks via Extracellular Vesicle-Packaged Let-7i-5p-Mediated Modulation of the MAPK Signaling Pathway. *Adv Sci*. 2022;9(3):e2102460. doi:10.1002/advs.202102460
42. Jun-Hao ET, Gupta RR, Shyh-Chang N. Lin28 and let-7 in the Metabolic Physiology of Aging. *Trends Endocrinol Metab*. 2016;27(3):132–141. doi:10.1016/j.tem.2015.12.006
43. Rybak A, Fuchs H, Smirnova L, et al. A feedback loop comprising lin-28 and let-7 controls pre-let-7 maturation during neural stem-cell commitment. *Nat Cell Biol*. 2008;10(8):987–993. doi:10.1038/ncb1759
44. Kobayashi T, Kozlova A. Lin28a overexpression reveals the role of Erk signaling in articular cartilage development. *Development*. 2018;145(15): dev162594. doi:10.1242/dev.162594
45. Jouan Y, Bouchemla Z, Bardèche-Trystram B, et al. Lin28a induces SOX9 and chondrocyte reprogramming via HMGA2 and blunts cartilage loss in mice. *Sci Adv*. 2022;8(34):eabn3106. doi:10.1126/sciadv.abn3106
46. Evans MA, Smart N, Dubé KN, et al. Thymosin β4-sulfoxide attenuates inflammatory cell infiltration and promotes cardiac wound healing. *Nat Commun*. 2013;4(1):2081. doi:10.1038/ncomms3081
47. Chang MY, Yang YS, Tsai ML, et al. Adenovirus-mediated prothymosin α gene transfer inhibits the development of atherosclerosis in ApoE-deficient mice. *Int J Biol Sci*. 2014;10(4):358–366. doi:10.7150/ijbs.8634
48. Halder SK, Matsunaga H, Ishii KJ, Ueda H. Prothymosin-alpha preconditioning activates TLR4-TRIF signaling to induce protection of ischemic retina. *J Neurochem*. 2015;135(6):1161–1177. doi:10.1111/jnc.13356
49. Gladka MM, Johansen AKZ, van Kampen SJ, et al. Thymosin β4 and prothymosin α promote cardiac regeneration post-ischaemic injury in mice. *Cardiovasc Res*. 2023;119(3):802–812. doi:10.1093/cvr/cvac155
50. Xu H, Li J, Fei Q, Jiang L. Contribution of immune cells to intervertebral disc degeneration and the potential of immunotherapy. *Connect Tissue Res*. 2023;64(5):413–427. doi:10.1080/03008207.2023.2212051
51. Wang G, Jin S, Ling X, et al. Proteomic Profiling of LPS-Induced Macrophage-Derived Exosomes Indicates Their Involvement in Acute Liver Injury. *Proteomics*. 2019;19(3):e1800274. doi:10.1002/pmic.201800274